

Journal of Materials Chemistry C

Accepted Manuscript



This is an *Accepted Manuscript*, which has been through the Royal Society of Chemistry peer review process and has been accepted for publication.

Accepted Manuscripts are published online shortly after acceptance, before technical editing, formatting and proof reading. Using this free service, authors can make their results available to the community, in citable form, before we publish the edited article. We will replace this *Accepted Manuscript* with the edited and formatted *Advance Article* as soon as it is available.

You can find more information about *Accepted Manuscripts* in the [Information for Authors](#).

Please note that technical editing may introduce minor changes to the text and/or graphics, which may alter content. The journal's standard [Terms & Conditions](#) and the [Ethical guidelines](#) still apply. In no event shall the Royal Society of Chemistry be held responsible for any errors or omissions in this *Accepted Manuscript* or any consequences arising from the use of any information it contains.

Light Blue and Green Thermally Activated Delayed Fluorescence from 10*H*-Phenoxaborin-Derivatives and Their Application to Organic Light-Emitting Diodes†

Received 00th January 20xx,
Accepted 00th January 20xx

DOI: 10.1039/x0xx00000x

www.rsc.org/

Yuichi Kitamoto,^{*a} Taketo Namikawa,^b Dai Ikemizu,^b Yasuo Miyata,^b Takatsugu Suzuki,^b Hiroshi Kita,^c Tetsuo Sato,^{a,d} and Shuichi Ojima^{*a}

New luminescent compounds consisting of 10*H*-phenoxaborinyl group as an electron-accepting unit and carbazole (**9**), 9,9-dimethylacridane (**10**), or phenoxazine (**11**) as an electron-donating unit have been synthesized. Compounds **10** and **11** showed thermally activated delayed fluorescence (TADF) with light blue and green emissions, respectively, with very high PL quantum yields (PLQYs), however, compound **9** exhibited only a prompt emission and no delayed component. Photoluminescence studies and quantum chemical calculation based on density functional theory (DFT) and time-dependent density functional theory (TD-DFT) revealed that in comparison with compound **9**, HOMO and LUMO for compounds **10** and **11** are well separated, resulting in lowering ΔE_{ST} and effective reverse intersystem crossing (RISC) between a lowest triplet excited state (T_1) and a lowest singlet excited state (S_1). Organic light-emitting diodes (OLEDs) using compounds **10** and **11** exhibited light blue and green emissions with very good maximum η_{ext} of 15.1% and 22.1%, respectively.

Introduction

After pioneering work on multilayer organic light-emitting diodes (OLEDs) by the research group of Eastman Kodak Ltd.,¹ OLEDs has been widely developed and applied to smart phones, flat-panel displays, and lighting applications² because they realized high efficiency,³ slim design, and flexible form.⁴ Under electrical excitation, 25% of singlet excitons and 75% of triplet excitons being formed by a spin statistic rule,⁵ early OLEDs using fluorescent materials exhibit theoretically at most 25% of internal quantum efficiency (η_{int}) with the triplet excitons wasted as a non-radiative decay. In order to improve η_{int} of the OLEDs, phosphorescent materials consisting of organic-heavy metal complexes have developed because intersystem crossing (ISC) from singlet excited states to triplet excited states and radiative triplet decay rates are effectively enhanced by high spin-orbit coupling induced by the heavy metal, resulting in theoretical 100% η_{int} .⁶ Fluorescent based OLEDs harvesting 75% triplet excitons have also been

demonstrated: triplet-triplet annihilation (TTA), which generate one singlet exciton by annihilative reaction between two triplet excitons, can totally generate a maximum 62.5% of singlet excitons.⁷ Hybridized local and charge-transfer (HLCT), which harvest triplet excitons via the reverse intersystem crossing (RISC) between high-lying triplet CT excited states (3CT_x) and singlet CT excited state (1CT_x), can realize theoretically 100% η_{int} .⁸ Recently, Adachi et al. have found that OLEDs doped Sn^{IV}-porphyrin complexes⁹ exhibited thermally activated delayed fluorescence that enable triplet excitons to up-convert to singlet excitons via endothermic RISC.¹⁰ As all of the excitons generated by electrical excitation can be converted into fluorescent luminescence, TADF materials such as cuprous complexes,¹¹ zinc complexes,¹² and metal-free organic molecules¹³⁻²⁰ have been developed in the past few years.

For an effective intersystem up-conversion of triplet excitons from T_1 state to S_1 state in TADF process, the energy gap between S_1 and T_1 , ΔE_{ST} , play a key role, which depends on the overlapping of the frontier molecular orbitals of a highest occupied molecular orbital (HOMO) and lowest unoccupied molecular orbital (LUMO).^{13a,21} This theory indicates that the spatial separation of the two orbitals leads to a lowering of ΔE_{ST} ,^{21a} which results in an efficient TADF. Adachi group has achieved metal-free TADF molecules with a small ΔE_{ST} and high external quantum efficiency (η_{ext}) by introducing donor and acceptor moieties with a suitable steric hindrance and distance, which enabled to develop efficient OLEDs without using expensive heavy metals, such as Ir and Pt.^{19b} Recently, boron-containing compounds exhibiting high electron mobility have jointly reported by Konica Minolta, Inc.

^a New Industry Creation Hatchery Center, Tohoku University, 6-6-11 Aramaki-Aoba, Aoba-ku, Sendai 980-8579, Japan. Email: kitamoto@orgsynth.che.tohoku.ac.jp, oishu@aporg.che.tohoku.ac.jp

^b Technology Research Group, Advanced Technology Center, Corporate R&D Headquarters, Konica Minolta, Inc., 2970 Ishikawa-Machi, Hachioji-shi, Tokyo 192-8505, Japan

^c Organic Materials Laboratories, Advanced Layers Business Unit, Konica Minolta, Inc., 2970 Ishikawa-Machi, Hachioji-shi, Tokyo 192-8505, Japan

^d Present address: Liberal Arts, Sendai National College of Technology, 48 Nodayama, Medeshima-Shiote, Natori-shi, Miyagi 981-1239, Japan

† Electronic Supplementary Information (ESI) available. See DOI: 10.1039/x0xx00000x

and Shirota group,^{22a} and Chujo group.^{22b} Since the electron mobility originated from a high electron accepting ability of the boron atom, we imagined that the aromatic moiety incorporating the boron atom into the π -conjugated system would serve as a new acceptor unit for a TADF molecule. Herein, we report new TADF molecules consisting of 10*H*-phenoxaborinyl group as an electron-accepting unit and diarylamine-derivatives as an electron-donating unit.²³

Results and discussion

Our strategy of molecular design on the boron-containing TADF compounds is shown in Figure 1: electron-accepting and -donating units are cross-linked through a phenylene bridge at the 1,4-positions. We choose 10*H*-phenoxaborin unit as an acceptor and carbazole, phenoxazine, or 9,9-dimethyl-9,10-dihydroacridine (9,9-dimethylacridane) as a donor. We supposed that these quasi anthracene and fluorene moieties would be twisted by the steric repulsion between the hydrogen atoms of the cross-linking phenylene, donor, and acceptor, resulting in effective spatial separation of the HOMO and LUMO and lowering ΔE_{ST} .

These molecules were synthesized according to Scheme 1. Triarylamine halides **4-6** were synthesized by Cu- or Pd-catalyzed cross-coupling of carbazole (**1**), phenoxazine (**2**), or 9,9-dimethylacridane (**3**) with 1,4-dihalobenzenes as the precursors of the donor units. 10*H*-Phenoxaborin-10-ol (**7**) and isopropyl alcohol were subjected to esterification reaction to synthesize the borinate ester **8** as an intermediate of the acceptor unit. The borinate ester **8** was used without purification because it was rapidly hydrolyzed under air. Then, subsequent reaction of lithium triarylamines, which were prepared from **4-6** and *n*-butyl lithium, with borinate ester **8** gave the corresponding N-B type products **9-11** in good yield.

The absorption and photoluminescence (PL) spectra of compounds **9-11** in toluene are shown in Figure 2. The N-B type compounds having carbazole (**9**), acridane (**10**), and phenoxazine (**11**) as a donor exhibited deep blue, light blue, and green emission at 300 K, respectively. The order of emission bands for fluorescence and phosphorescence also maintained at 77 K. The fluorescence bands of compounds **10** and **11** especially showed broad bands, suggesting that the emission originate from the intramolecular CT excitons. Comparing the fluorescence and phosphorescence emissions of compound **9** at 77 K, the difference in two onsets of the emissions was 40.9 nm and the value of ΔE_{ST} was experimentally estimated to be 0.35 eV.²⁴ On the other hand, the fluorescence bands of compounds

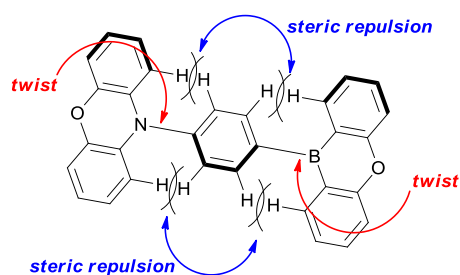
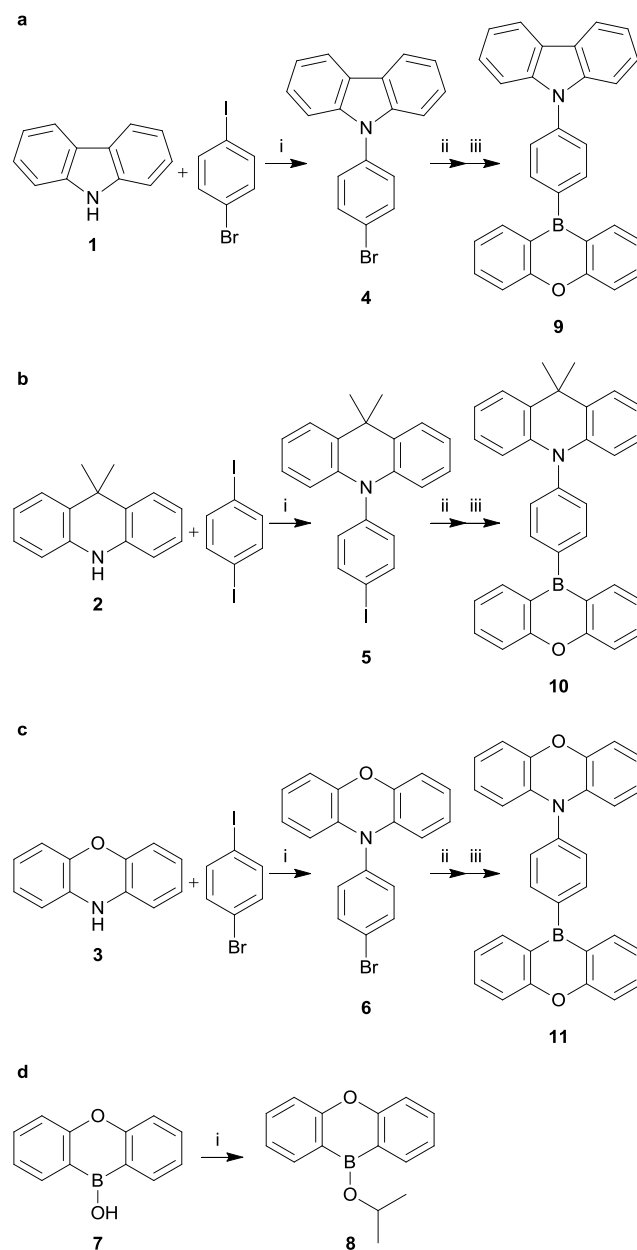


Fig. 1 Molecular design of boron-based TADF molecules.



Scheme 1 Synthesis of compounds **9-11**: a) i) CuI, LiCl, Cs₂CO₃, DMF, microwave, 220 °C; ii) *n*-BuLi, THF-Et₂O, -78 °C; iii) borinate ester **8**, THF-Et₂O, -78 °C; b) i) CuI, KI, Cs₂CO₃, DMF, microwave 220 °C; ii) *n*-BuLi, THF-Et₂O, -78 °C; iii) borinate ester **8**, THF-Et₂O, -78 °C; c) i) Pd₂(dba)₃·CHCl₃, JohnPhos, NaO^tBu, toluene, 60 °C; ii) *n*-BuLi, THF-Et₂O, -78 °C; iii) borinate ester **8**, THF-Et₂O, -78 °C; d) i) isopropyl alcohol-benzene, MS3A, reflux.

10 and **11** were very close to the phosphorescence bands and their experimental values of ΔE_{ST} were determined to be 0.013 and 0.028 eV, respectively. The small ΔE_{ST} of compounds **10** and **11** suggests that these two N-B type molecules, which have quasi anthracene skeletons as donors, exhibit efficient TADF in comparison to compound **9** having a quasi fluorene skeleton as a donor.

To elucidate the delayed fluorescence from the N-B type compounds, we analyzed the PL characteristics of polystyrene film fabricated with 6 wt% of compounds **9**, **10** and **11** by wet

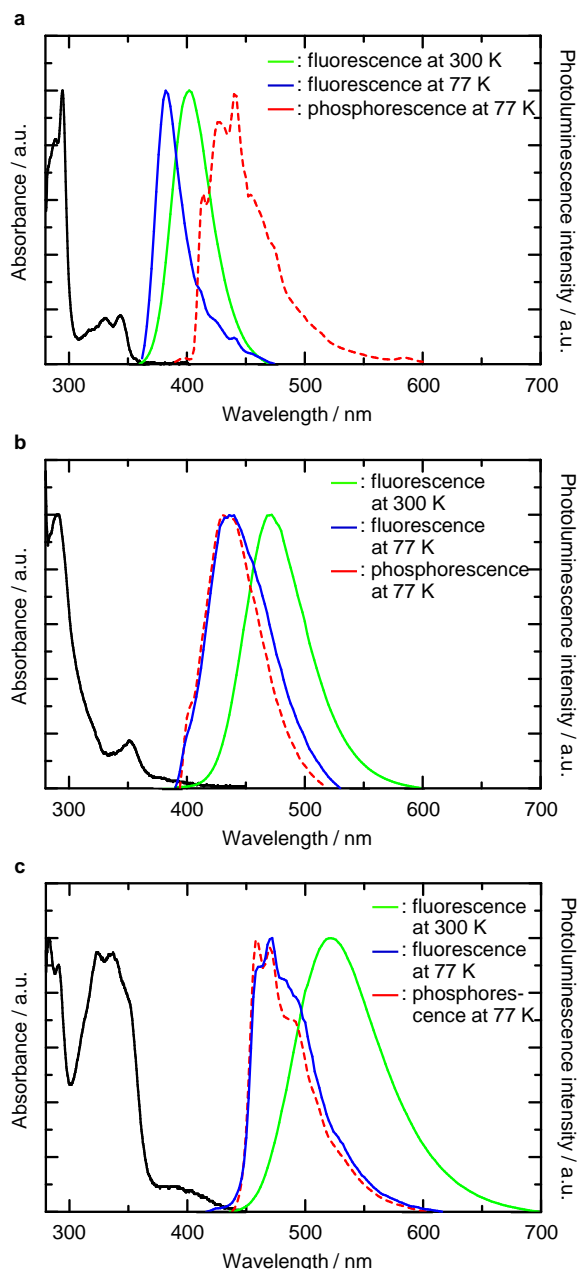


Fig. 2 Absorption and fluorescence spectra of a) compound **9**, b) **10**, and c) **11** in toluene (ex. 290 nm). Green and blue lines represent fluorescence spectra at 300 K and 77 K, respectively. Black line represents UV-vis spectra. Red dotted line represents phosphorescence spectra at 77 K.

process using a streak camera at 300 K under N_2 . Figure 3 shows transient PL decay curves and the prompt and delayed PL spectra. The PL curves of compounds **10** and **11** are comprised of sharp and gently-sloping emissions, which are attributed to prompt and delayed components, respectively. In addition, the prompt emission bands for compounds **10** and **11** coincide with the delayed emission bands with peak position at 440 and 482 nm, respectively (inset figures in Figure 3b and 3c). These results strongly indicate that the fabricated films with compounds **10** and **11** exhibit TADF emissions. Fitting

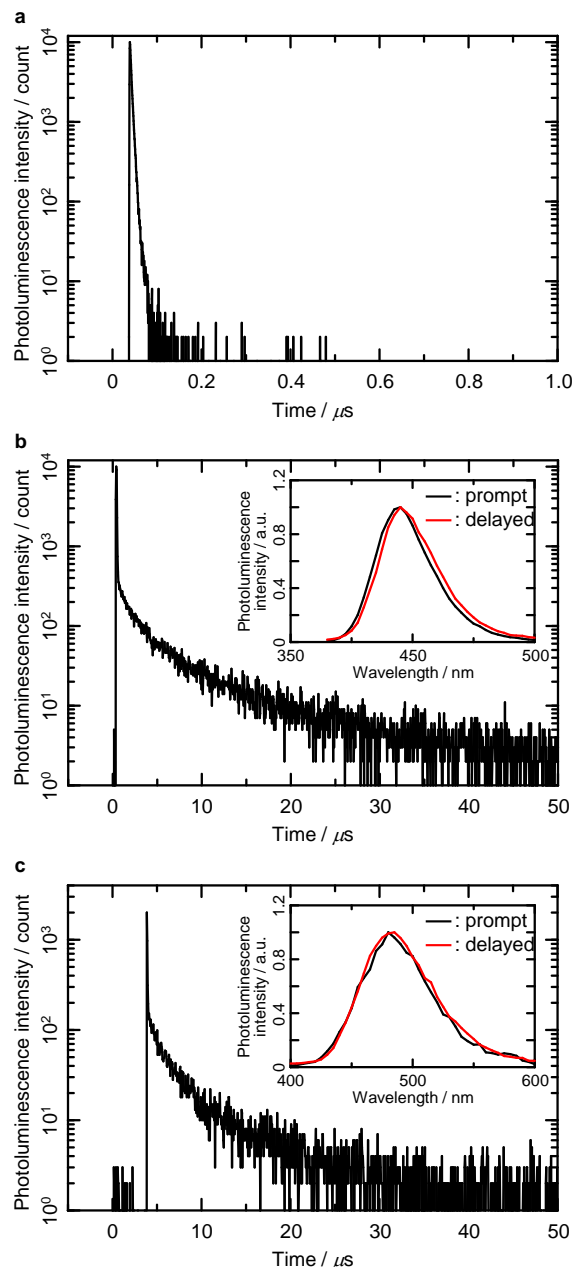


Fig. 3 Transient photoluminescence of 6 wt% a) compounds **9**, b) **10**, and c) **11**: polystyrene films fabricated by wet process (Yag laser, $\lambda = 355$ nm). The inset shows prompt (black line) and delayed (red line) photoluminescence spectra of 6 wt% **10** and **11**: polystyrene fabricated films.

four- and three-exponentials for compounds **10** and **11**, the weight-average lifetimes are determined to be 2.36 and 1.87 μs , respectively, showing the effective RISC process occurs. These short-lived TADF emissions are suitable for OLED emitters because long-lived emissions relating to triplets excitons could cause the triplet-triplet and singlet-triplet annihilations, resulting in quantum efficiency roll-off.^{17b,25} In contrast with compounds **10** and **11**, the carbazole-based molecule **9** exhibited only a prompt emission and showed no delayed component.

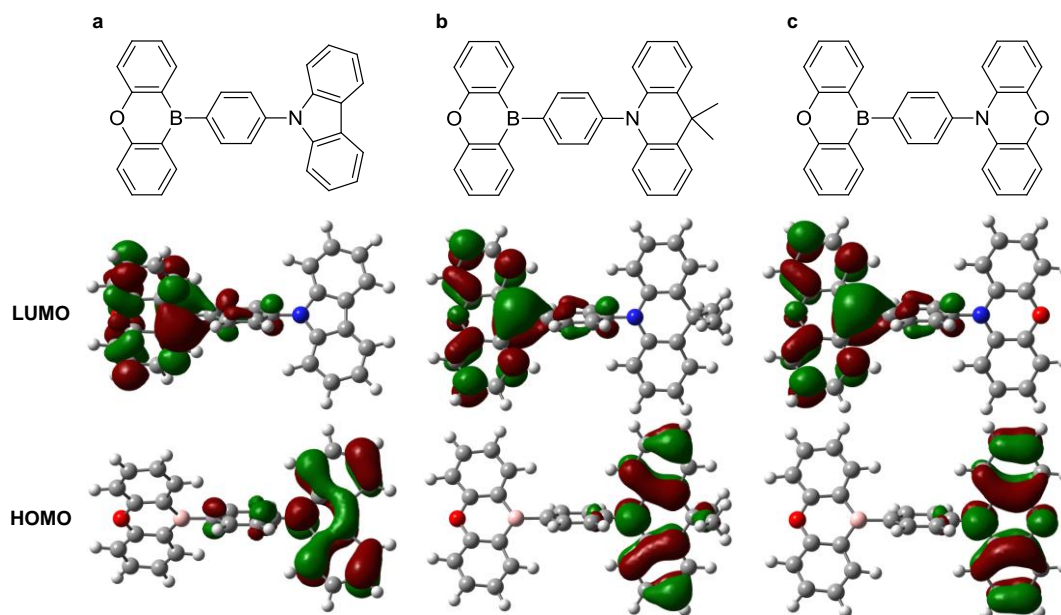


Fig. 4 The HOMO and LUMO distribution of a) compounds **9**, b) **10**, and c) **11** calculated at the M06/6-31G* level.^{26b}

In order to clarify why the TADF characteristics were observed for the phenoxazine- and acridane-based molecules but not the carbazole-based molecule, quantum chemical calculations for S_0 states of compounds **9-11** were carried out using density functional theory (DFT) at the M06/6-31G* level.²⁶ Figure 4 shows the optimized structures and the HOMO and LUMO of compounds **9-11**. The dihedral angle between the phenylene and the acceptor of compound **9** ($\theta = 53.6^\circ$) is almost the same as that of compounds **10** and **11** ($\theta = 51.8, 52.2^\circ$, respectively). On the other hand, the dihedral angles between the phenylene and the donors are largely different: for compounds **10** and **11**, the dihedral angles are calculated to be 88.9 and 87.5, respectively, while compound **9** exhibits much smaller dihedral angle of 54.7°. For compounds **9-11**, the LUMO is mainly distributed on the 10*H*-phenoxaborin moiety, which indicates that the π -conjugated moiety containing boron atom serve as an acceptor. The HOMO of compounds **10** and **11** are well-separated spatially on the donors, but the HOMO of compound **9** is predominantly localized not only on the donor but also on the cross-linking phenylene moiety adjacent to the acceptor. These differences in the dihedral angles and degree of orbital overlap were assumed to affect the value of ΔE_{ST} . We next calculated the S_1 and T_1 excited energies at the ground state (S_0) of compounds **9-11** using time-dependent density functional theory (TD-DFT) at the M06/6-31G* level.²⁶⁻²⁸ It was found that compounds **10** and **11** exhibit very small energy gaps between S_1 and T_1 ($\Delta E(S_1-T_1@S_0)$) of 0.0027 and 0.0036 eV, respectively, which are much smaller than that of compound **9** (0.295 eV). This correlation of calculated $\Delta E(S_1-T_1@S_0)$ shows similar tendency with the experimental ΔE_{ST} of compounds **9-11** (*vide supra*). Although the optimization of excited states for each molecule was not performed in the present study, these DFT and TD-DFT calculations give us the important information about the relationship between the

molecular structure and ΔE_{ST} . On the basis of these observation and calculation, the value of ΔE_{ST} is dependent on the molecular structure of donor and the twist angle between the donor and cross-linking phenylene: for compounds **10** and **11** having acridane and phenoxazine as a donor, the steric repulsion between the hydrogen atoms of the donor and cross-linking phenylene causes the large dihedral angles as shown in Figure 1. For compound **9** having carbazole as a donor, on the other hand, the relative small five-membered ring decrease the steric repulsion, resulting in the decrease of the dihedral angle, overlapping of the HOMO and LUMO, and making the ΔE_{ST} larger than that of **10** and **11**.

To evaluate the performance of compounds **10** and **11** as an emitter in OLEDs, we examined the electroluminescence (EL) characteristics of multilayer OLEDs using compounds **10** and **11** as the emitters as follows: the device structures are

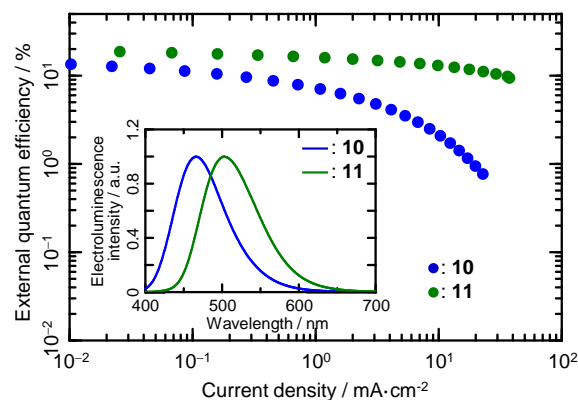


Fig. 5 The external quantum efficiency-current density characteristic of the OLEDs using compounds **10** and **11**. The inset shows the electroluminescence spectra. The blue and green plots represent compounds **10** and **11**, respectively.

ITO/PEDOT:PSS (40 nm)/ α -NPD (35 nm)/mCP (10 nm)/compound **10** (6%):DPEPO (20 nm)/DPEPO (10 nm)/TPBi (40 nm)/Al (100 nm) and ITO/PEDOT:PSS (40 nm)/ α -NPD (35 nm)/mCP (10 nm)/compound **11** (6%):mCP (20 nm)/PPT (10 nm)/TPBi (40 nm)/LiF (0.5 nm)/Al (100 nm) (Figure S1). For compounds **10** and **11**, the devices exhibited light blue and green EL with the peak positions of the EL spectra at 466 and 503 nm with very good maximum η_{ext} of 15.1 and 22.1%, respectively (Figure 5). These results clearly indicate that the substantial triplet excitons contribute the luminescence. The PL quantum yields (PLQYs) of 6 wt% doped film of compounds **10** and **11** in the corresponding host layers under nitrogen were then measured. Compound **10** in DPEPO and **11** in mCP showed very high PLQYs of 98% (excited at 300 nm) and 99% (excited at 320 nm), respectively. Considering a light outcoupling efficiency of 20–30%, an estimated electroluminescence η_{int} of **11** is as high as its PLQY. In comparison to this, a decline of the electroluminescence η_{ext} of **10**, in spite of the high PLQY as **11**, indicates that there is room to improve the choice of the host compound and the

OLED layer structure.

We found that for the devices using compounds **10** and **11**, current density vs. luminescence plots did not exhibit a quadratic increase but a liner increase (Figure 6), indicating that the processes of the luminescence from the triplet excitons are not the TTA mode but the TADF mode.^{15b,29} It is also noted that the device based on **10** exhibits a high luminescence of 8216 $\text{cd}\cdot\text{m}^{-2}$ at 8.5 V as shown in Figure 7 and maintains a high η_{ext} of 14.6% even at a luminescence of 1000 $\text{cd}\cdot\text{m}^{-2}$. These EL characteristics are caused by the small ΔE_{ST} and the short life time of the excitons of the boron containing TADF molecules **10** and **11**.

Conclusions

In summary, we have demonstrated light blue and green TADF molecules consisting of the π -conjugated system containing boron atom as an electron-accepting unit and diarylamine derivatives as an electron-donating unit. For compounds **10** and **11**, phenoxazine and acridane moieties induced suitable twists between the donors and the cross-linking phenylene, resulting in a very small ΔE_{ST} and short-lived TADF emissions. OLEDs constructed with **10** and **11** as dopants exhibited high η_{ext} and luminescence, indicating that these molecules are promising candidate for dopants of OLEDs. Further optimization of the dopant molecular structure as well as the host compound and

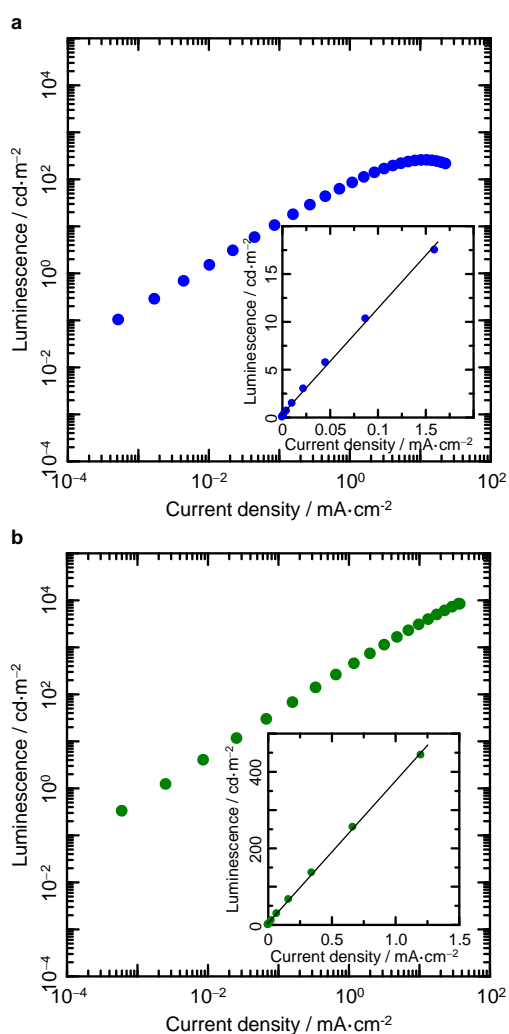


Fig. 6 Luminance-current density characteristics of the OLEDs using a) compounds **10**, and b) **11** as an emitter. The inset show luminescence-current density characteristics at the region with low current density. The blue and green plots represent compound **10** and **11**, respectively.

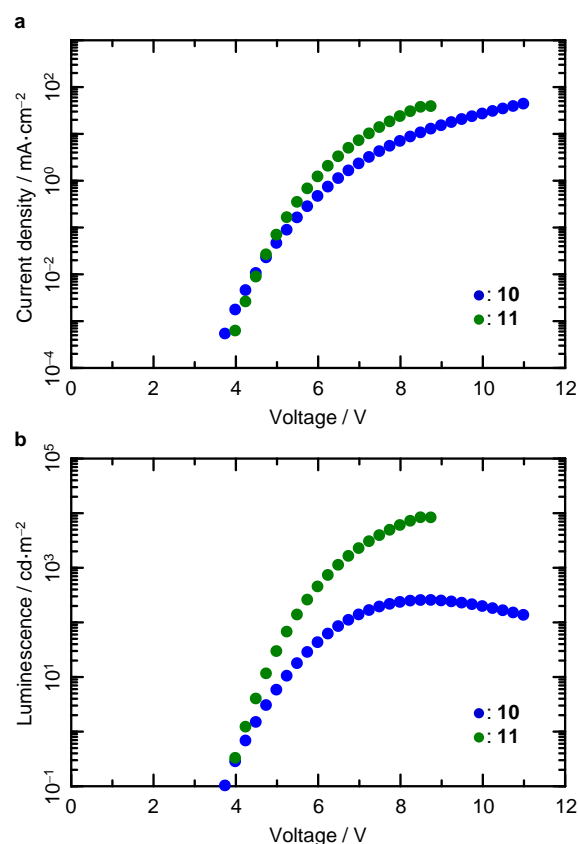


Fig. 7 The OLEDs characteristics using compounds **10**, and **11** as an emitter: a) Current density-voltage characteristics, and b) luminescence-voltage characteristics. The blue and green plots represent compound **10** and **11**, respectively.

the multilayer structure would contribute to improve blue-emitting OLEDs using TADF molecules with boron atom.

Experimental

General

NMR spectra were recorded on an AVANCE III 400 spectrometer. ^1H NMR were obtained at 400 MHz and referenced to tetramethylsilane singlet at 0.00 ppm. ^{13}C NMR were obtained at 100 MHz and referenced to the center line of the CDCl_3 triplet and $\text{DMSO-}d_6$ octet at 77.16 and 39.52 ppm. ^{11}B NMR were obtained at 128 MHz and referenced to $\text{BF}_3\cdot\text{OEt}$ at 0.00 ppm as an external standard. High-resolution mass spectra were obtained on a JEOL JMS-700 spectrometer at the Department of Instrumental Analysis of the Technical Division, School of Engineering, Tohoku University. IR spectra were recorded on a JASCO FT/IR-350 Fourier-transform infrared spectrometer. Photoluminescence spectra in toluene were recorded on a Hitachi High-Tech F-7000 Spectrophotometer. UV-vis spectra in toluene were recorded on Shimadzu UV-2500 spectrophotometer. Melting points were recorded using a Stuart melting point apparatus SMP3. The transient photoluminescence decay of the films fabricated with TADF molecules were recorded using a Hamamatsu Photonics Quantaaurus-Tau C11367-01 equipped with YaG laser ($\lambda = 355$ nm). The prompt and delayed emission spectra were also recorded using a Hamamatsu Photonics Quantaaurus-Tau C11367-01 equipped with YaG laser ($\lambda = 355$ nm). PL quantum efficiencies were measured using a Hamamatsu Photonics Quantaaurus-QY C11347-01 absolute photoluminescence quantum yield measurement system. The electroluminescence spectra and current density-voltage-luminance characteristics of the OLEDs were measured using a Konica Minolta CS-2000 Spectroradiometer, and an ADC DC Voltage and Current Source/Monitor.

All reactions were performed under a N_2 atmosphere in egg-plant shaped flasks unless noted otherwise. Microwave-assisted reactions were carried out with a Biotage Initiator+ Sixty (400 W, 2.45 GHz) using a Biotage 5 mL vial sealed with a crimp cap. Column chromatography was performed using spherical silica gel (63–200 μm , Kanto Chemical). Recycling preparative GPC was performed using preparative columns connecting a JAI JAIGEL-1H column (600 mm \times 20 mm i.d.) and a JAI JAIGEL-2H column (600 mm \times 20 mm i.d.) in series with CHCl_3 as an eluent.

Materials

All solvents (including super-dehydrated) using in reactions, UV-vis, and photoluminescence measurements was purchased and used as received. Commercially available reagents were purchased and used without purification unless noted otherwise.

10*H*-Phenoxaborin-10-ol (7).³⁰ **7** was prepared according to the literature procedures. White, fluffy solids, ^1H NMR (400 MHz, $\text{DMSO-}d_6$) δ 7.30 (ddd, 2H, $J = 7.5, 7.4, 0.90$ Hz), 7.44 (d, 2H, $J = 7.9$ Hz), 7.68 (ddd, 2H, $J = 7.9, 7.5, 1.7$ Hz), 8.16 (dd, 2H, $J = 7.4, 1.7$ Hz), 9.88 (brs, 1H); ^{13}C NMR (100 MHz,

$\text{DMSO-}d_6$) δ 17.1, 120.3, 122.2, 132.0, 133.3, 160.8; ^{11}B NMR (128 MHz, $\text{DMSO-}d_6$) δ 37.9; HRMS (FAB) calcd for $\text{C}_{12}\text{H}_9\text{BO}_2$ $[\text{M}]^+$ 196.0696, found 196.0697.

9-(4-Bromophenyl)-9*H*-carbazole (4).³¹ **4** was prepared according to the literature procedures. A white powder, ^1H NMR (400 MHz, CDCl_3) δ 7.29 (ddd, 2H, $J = 7.5, 7.2, 1.2$ Hz), 7.36–7.41 (m, 4H), 7.44 (d, 2H, $J = 8.7$ Hz), 7.72 (d, 2H, $J = 8.7$ Hz), 8.13 (d, 2H, $J = 7.5$ Hz); ^{13}C NMR (100 MHz, CDCl_3) δ 109.7, 120.3, 120.5, 121.0, 123.6, 126.2, 128.8, 133.2, 136.9, 140.7; HRMS (FAB) calcd for $\text{C}_{18}\text{H}_{12}\text{BrN}$ $[\text{M}]^+$ 321.0153, found 321.0152.

9-(4-(10*H*-phenoxaboryl)phenyl)-9*H*-carbazole (9). A 100 mL two-necked flask equipped with dropping funnel filled with MS3A and dimroth condenser was charged with **7** (166 mg, 1.0 equiv, 8.49×10^{-1} mmol), and then evacuated with heating and refilled with N_2 . 50 mL of dry 2-propanol and 10 mL of dry benzene were added and the reaction mixture was refluxed for 48 h. After the solvent was removed in *vacuo* at 70 $^\circ\text{C}$ for 2 h, the residue was dissolved with dry Et_2O and THF (2 mL and 4 mL, respectively) to give a solution of the borinate ester **8**. A 50 mL two-necked flask was charged with **4** (273 mg, 8.49×10^{-1} mmol), and then evacuated with heating and refilled with N_2 . 4 mL of dry THF and 3 mL of dry Et_2O were added, and then *n*-butyllithium (640 μL , 1.2 equiv, 1.02 mmol, 1.6 M in *n*-hexane) was added dropwise to the stirred solution at -78 $^\circ\text{C}$. The reaction mixture was stirred for 1.0 h at -78 $^\circ\text{C}$ and then the prepared solution of the borinate ester was added dropwise at -78 $^\circ\text{C}$. After stirring at -78 $^\circ\text{C}$ for 0.5 h, the solution was gradually warmed to room temperature and stirred for 24 h at room temperature. The resulting mixture was passed through a silica gel short column (dichloromethane). After the volatile was removed in *vacuo*, the product was recrystallized from dichloromethane–*n*-pentane at 0 $^\circ\text{C}$. After filtration and washing with *n*-pentane, the product **9** (178 mg, 58% yield) was obtained as white powder. Mp 232.0–233.5 $^\circ\text{C}$; IR (KBr) 3020.0, 2986.4, 1592.9, 1575.6, 1476.2, 1449.2, 1431.9, 1333.5, 1316.2, 1294.0, 1263.2, 1226.5, 910.2, 745.4, 721.3; ^1H NMR (400 MHz, CDCl_3) δ 7.32 (ddd, 2H, $J = 7.4, 7.4, 0.9$ Hz), 7.38 (ddd, 2H, $J = 7.8, 7.4, 1.0$ Hz), 7.47 (ddd, 2H, $J = 7.7, 7.6, 1.2$ Hz), 7.61 (d, 2H, $J = 7.8$ Hz), 7.66 (d, 2H, $J = 7.8$ Hz), 7.77 (d, 2H, $J = 8.3$ Hz), 7.81 (ddd, 2H, $J = 7.8, 7.7, 1.6$ Hz), 7.96 (d, 2H, $J = 8.3$ Hz), 8.17 (dd, $J = 7.6, 1.6$ Hz), 8.19 (d, 2H, $J = 7.4$ Hz); ^{13}C NMR (100 MHz, CDCl_3) δ 110.2, 118.0, 120.1, 120.5, 122.7, 123.7, 124.7, 126.1, 126.3, 134.8, 135.2, 136.6, 138.1, 139.8, 141.0, 160.2; ^{11}B NMR (128 MHz, CHCl_3) δ 51.3; HRMS (FAB) calcd for $\text{C}_{30}\text{H}_{20}\text{BNO}$ $[\text{M}]^+$ 421.1638, found 421.1635.

9,9-Dimethyl-9,10-dihydroacridine (2).³² **2** was prepared according to the literature procedures. A white powder, ^1H NMR (400 MHz, CDCl_3) δ 1.57 (s, 6H), 6.10 (brs, 1H), 6.67 (dd, 2H, $J = 7.7, 1.3$ Hz), 6.91 (ddd, 2H, $J = 7.7, 7.4, 1.3$ Hz), 7.09 (ddd, 2H, $J = 7.7, 7.4, 1.3$ Hz), 7.37 (dd, 2H, $J = 7.7, 1.3$ Hz); ^{13}C NMR (100 MHz, CDCl_3) δ 30.7, 36.3, 113.5, 120.7, 125.6, 126.9, 129.3, 138.6; HRMS (FAB) calcd for $\text{C}_{15}\text{H}_{15}\text{N}$ $[\text{M}]^+$ 209.1204, found 209.1206.

9,9-Dimethyl-10-(4-iodophenyl)-9,10-dihydroacridine (5). A 5 mL vial was charged with **2** (209 mg, 1.00 mmol), 1,4-

diiodobenzene (657 mg, 2.0 equiv, 2.00 mmol), CuI (189 mg, 1.0 equiv, 1.00 mmol), Cs₂CO₃ (327 mg, 1.0 equiv, 1.00 mmol), KI (332 mg, 2.0 equiv, 2.00 mmol), and dry DMF (2.4 mL). The vial was sealed with a crimp cap, and then the reaction was heated in the microwave reactor at 220 °C for 30 min. After the reaction mixture was diluted with dichloromethane, the resulting solution was passed through a celite short column (dichloromethane). The resulting mixture was washed successively with sat. NH₄Cl aq. and brine, dried over MgSO₄, and evaporated. The residue was purified by silica gel chromatography with hexane-dichloromethane (7:1) as an eluent to give the product **5** (295 mg, 72% yield) as white crystalline solids. Mp 165.8–166.7 °C; IR (KBr) 3075.9, 2943.2, 1586.2, 1498.4, 1470.5, 1449.2, 1322.0, 1268.9, 1008.6, 744.4; ¹H NMR (400 MHz, CDCl₃) δ 1.67 (s, 6H), 6.25 (dd, 2H, *J* = 7.8, 1.5 Hz), 6.93 (2H, ddd, *J* = 7.5, 7.4, 1.5 Hz), 6.97 (2H, ddd, *J* = 7.8, 7.5, 1.8 Hz), 7.09 (2H, d, *J* = 8.5 Hz), 7.45 (2H, dd, *J* = 7.4, 1.8 Hz), 7.95 (2H, d, *J* = 8.5 Hz); ¹³C NMR (100 MHz, CDCl₃) δ 31.4, 36.1, 93.8, 114.1, 120.9, 125.5, 126.5, 130.2, 133.7, 140.4, 140.7, 141.2; HRMS (FAB) calcd for C₂₁H₁₈IN [M]⁺ 411.0484, found 411.0490.

9,9-Dimethyl-10-(4-(10H-phenoxaboryl)phenyl)-9,10-dihydroacridine (10). A solution of borinate ester **8** was prepared as above using 204 mg (1.0 equiv, 1.04 mmol) of **7**. A 50 mL two-necked flask was charged with **5** (427 mg, 1.0 equiv, 1.04 mmol), and evacuated with heating and refilled with N₂. 4.5 mL of dry THF and 4.5 mL of dry Et₂O were added, and then *n*-butyllithium (780 μL, 1.2 equiv, 1.25 mmol, 1.6 M in *n*-hexane) was added dropwise to the stirred solution at –78 °C. The reaction mixture was stirred for 1.5 h at –78 °C and then the prepared solution of **8** was added dropwise at –78 °C. After stirring at –78 °C for 0.5 h, the solution was gradually warmed to room temperature and stirred for 24 h at room temperature. The resulting mixture was passed through a silica gel short column (dichloromethane). After volatile was removed in *vacuo*, the residue was purified by recycling preparative GPC. After the volatile was removed in *vacuo*, the product was recrystallized from dichloromethane–*n*-pentane at 0 °C. After filtration and washing with *n*-pentane, the product **10** (305 mg, 65% yield) was obtained as pale light blue crystals. Mp 195.9–197.1 °C; IR (KBr) 3065.3, 2931.8, 1590.0, 1573.6, 1475.3, 1431.9, 1334.5, 1266.0, 1205.3, 1135.9, 911.2, 745.4; ¹H NMR (400 MHz, CDCl₃) δ 1.73 (s, 6H), 6.47 (dd, 2H, *J* = 7.9, 1.0 Hz), 6.96 (ddd, 2H, *J* = 7.6, 7.5, 1.0 Hz), 7.05 (ddd, 2H, *J* = 7.9, 7.5, 1.5 Hz), 7.38 (t, 2H, *J* = 7.6 Hz), 7.49 (dd, 2H, *J* = 7.6, 1.5 Hz), 7.52 (d, 2H, *J* = 8.1 Hz), 7.65 (d, 2H, *J* = 8.0 Hz), 7.80 (ddd, 2H, *J* = 8.0, 7.6, 1.6 Hz), 7.97 (d, 2H, *J* = 8.1 Hz), 8.16 (dd, 2H, *J* = 7.6, 1.6 Hz); ¹³C NMR (100 MHz, CDCl₃) δ 31.3, 36.2, 114.3, 118.0, 120.7, 122.7, 124.7, 125.3, 126.5, 130.2, 130.6, 134.9, 136.2, 136.6, 140.7, 141.2, 141.6, 160.2; ¹¹B NMR (128 MHz, CHCl₃) δ 50.6; HRMS (FAB) calcd for C₃₃H₂₆BNO [M]⁺ 463.2107, found 463.2106.

10-(4-Bromophenyl)-10H-phenoxazine (6). A 100 mL two-necked flask was equipped with Pd₂(dba)₃·CHCl₃ (21 mg, 2.0 mol%, 2.00×10^{–2} mmol), 2-(di-*tert*-butylphosphino)biphenyl (18 mg, 6.0 mol%, 6.00×10^{–2} mmol), and NaO^tBu (289 mg, 3.0 equiv, 3.00 mmol), and then

evacuated and refilled with N₂. 1.5 mL of dry toluene was added and the reaction mixture was stirred at 60 °C until a dark purplish-red persisted (for ca. 5 min). 10H-phenoxazine **3** (183 mg, 1.00 mmol), 1-bromo-4-iodobenzene (706 mg, 2.5 equiv, 2.50 mmol), and dry toluene (1.5 mL) were added, and then the reaction was stirred at 60 °C for 11 h. After the reaction mixture was diluted with dichloromethane, the resulting solution was passed through a celite short column (dichloromethane). The resulting mixture was washed successively with sat. NH₄Cl aq. and brine, dried over MgSO₄, and evaporated. The residue was purified by silica gel chromatography with hexane-dichloromethane (6:1) as an eluent to give the product **6** (272 mg, 81% yield) as white crystalline solids. Mp 196.5–197.9 °C; IR (KBr) 3045.5, 2886.4, 1590.0, 1483.0, 1335.5, 1291.1, 1272.8, 1208.2, 1010.5, 736.7; ¹H NMR (400 MHz, CDCl₃) δ 5.91 (dd, 2H, *J* = 7.8, 1.4 Hz), 6.57–6.70 (m, 6H), 7.23 (d, 2H, *J* = 8.6 Hz), 7.72 (d, 2H, *J* = 8.6 Hz); ¹³C NMR (100 MHz, CDCl₃) δ 113.3, 115.7, 121.7, 122.5, 123.4, 132.9, 134.1, 134.6, 138.2, 144.0; HRMS (FAB) calcd for C₁₈H₁₂BrNO [M]⁺ 337.0102, found 337.0104.

10-(4-(10H-phenoxaboryl)phenyl)-10H-phenoxazine (11). A solution of borinate ester **8** was prepared as above using 182 mg (1.0 equiv, 9.31×10^{–1} mmol) of **7**. A 50 mL two-necked flask was charged with **6** (314 mg, 9.31×10^{–1} mmol), and then evacuated with heating and refilled with N₂. 4.5 mL of dry THF and 2 mL of dry Et₂O were added, and then *n*-butyllithium (700 μL, 1.2 equiv, 1.11 mmol, 1.6 M in *n*-hexane) was added dropwise to the stirred solution at –78 °C. The reaction mixture was stirred for 1.5 h at –78 °C and then the prepared solution of **8** was added dropwise at –78 °C. After stirring at –78 °C for 0.5 h, the solution was gradually warmed to room temperature and stirred for 24 h at room temperature. The resulting mixture was passed through a silica gel short column (dichloromethane). After the volatile was removed in *vacuo*, the product was recrystallized from ethylacetate–*n*-hexane at 0 °C. After filtration and washing with *n*-pentane, the product **11** (265 mg, 65% yield) was obtained as blight yellow crystals. Mp 242.5–244.4 °C; IR (KBr) 3061.4, 2981.8, 1589.1, 1576.5, 1487.8, 1449.2, 1431.9, 1333.5, 1294.0, 1272.8, 1208.2, 910.2, 759.8, 737.6; ¹H NMR (400 MHz, CDCl₃) δ 6.10 (br, 2H), 6.66–6.73 (m, 6H), 7.37 (ddd, 2H, *J* = 7.6, 7.5, 0.73 Hz), 7.52 (d, 2H, *J* = 8.0 Hz), 7.65 (dd, 2H, *J* = 8.1, 0.73 Hz), 7.80 (ddd, 2H, *J* = 8.1, 7.6, 1.7 Hz), 7.94 (d, 2H, *J* = 8.0 Hz), 8.10 (dd, 2H, *J* = 7.5, 1.7 Hz); ¹³C NMR (100 MHz, CDCl₃) δ 113.5, 115.6, 118.0, 121.5, 122.7, 123.4, 124.6, 130.1, 134.6, 134.9, 136.3, 136.5, 139.3, 141.1, 144.2, 160.2; ¹¹B NMR (128 MHz, CHCl₃) δ 50.3; HRMS (FAB) calcd for C₃₀H₂₀BNO₂ [M]⁺ 437.1587, found 437.1587.

Acknowledgements

We thank Prof. T. Hattori (Tohoku University) for courteous permission to use their instruments and technical guidance.

Notes and references

- 1 C. W. Tang and S. A. VanSlyke, *Appl. Phys. Lett.*, 1987, **51**, 913–915.
- 2 Reviews: (a) B. W. D'Andrade and S. R. Forrest, *Adv. Mater.*, 2004, **16**, 1585–1595; (b) H. Yersin, *Highly Efficient OLEDs with Phosphorescent Materials*, Wiley-VCH, Weinheim, 2008; (c) M. C. Gather, A. Köhnen and K. Meerholz, *Adv. Mater.*, 2011, **23**, 233–248; (d) W. Brütting and C. Adachi, *Physics of Organic Semiconductors*, Wiley-VCH, Weinheim, 2nd edn., 2012; (e) N. Thejo Kalyani and S. J. Dhoble, *Renew. Sustain. Energy Rev.*, 2012, **16**, 2696–2723; (f) A. Buckley, *Organic light-emitting diodes (OLEDs): Materials, devices and applications*, Woodhead Publishing, Cambridge, 2013.
- 3 (a) T. Nakayama, K. Hiyama, K. Furukawa and H. Ohtani, *J. Soc. Info. Dis.*, 2008, **16**, 231–236; (b) S. Reineke, F. Lindner, G. Schwartz, N. Seidler, K. Walzer, B. Lüssem and K. Leo, *Nature*, 2009, **459**, 234–238; (c) K. Hiyama, H. Ito, Y. Okubo and H. Kita, *SID. Int. Symp. Dig. Tech.*, 2014, **45**, 679–281.
- 4 (a) S. Kim, H. -J. Kwon, S. Lee, H. Shim, Y. Chun, W. Choi, J. Kwack, D. Han, M. Song, S. Kim, S. Mohammadai, I. Kee and S. Y. Lee, *Adv. Mater.*, 2011, **23**, 3511–3516; (b) Z. Yu, X. Niu, Z. Liu and Q. Pei, *Adv. Mater.*, 2011, **23**, 3989–3994.
- 5 (a) M. A. Baldo, D. F. O'Brien, M. E. Thompson and S. R. Forrest, *Phys. Rev. B: Condens. Matter Mater. Phys.*, 1999, **60**, 14422–14428; (b) M. Segal, M. A. Baldo, R. J. Holmes, S. R. Forrest and Z. G. Soos, *Phys. Rev. B: Condens. Matter Mater. Phys.*, 2003, **68**, 075211.
- 6 (a) M. A. Baldo, D. F. O'Brien, Y. You, A. Shoustikov, S. Sibley, M. E. Thompson and S. R. Forrest, *Nature*, 1998, **395**, 151–154; (b) C. Adachi, M. A. Baldo, M. E. Thompson and S. R. Forrest, *J. Appl. Phys.*, 2001, **90**, 5048–5051.
- 7 (a) C. T. Brown and D. Kondakov, *J. Soc. Info. Dis.*, 2004, **12**, 323–327; (b) D. Y. Kondakov, T. D. Pawlik, T. K. Hatwar and J. P. Spindler, *J. Appl. Phys.*, 2009, **106**, 124510; (c) C. -J. Chiang, A. Kimyonok, M. K. Etherington, G. C. Griffiths, V. Jankus, F. Turksoy and A. P. Monkman, *Adv. Funct. Mater.*, 2013, **23**, 739–746.
- 8 (a) W. Li, D. Liu, F. Shen, D. Ma, Z. Wang, T. Feng, Y. Xu, B. Yang and Y. Ma, *Adv. Funct. Mater.*, 2012, **22**, 2797–2803; (b) L. Yao, S. Zhang, R. Wang, W. Li, F. Shen, B. Yang and Y. Ma, *Angew. Chem. Int. Ed.*, 2014, **53**, 2119–2123.
- 9 First example of an application of TADF process to OLEDs, see: A. Endo, M. Ogasawara, A. Takahashi, D. Yokoyama, Y. Kato and C. Adachi, *Adv. Mater.*, 2009, **21**, 4802–4806.
- 10 Review : Y. Tao, K. Yuan, T. Chen, P. Xu, H. Li, R. Chen, C. Zheng, L. Zhang and W. Huang, *Adv. Mater.*, 2014, **26**, 7931–7958.
- 11 (a) J. C. Deaton, S. C. Switalski, D. Y. Kondakov, R. H. Young, T. D. Pawlik, D. J. Giesen, S. B. Harkins, A. J. M. Miller, S. F. Mickenberg and J. C. Peters, *J. Am. Chem. Soc.*, 2010, **132**, 9499–9508; (b) R. Czerwieńiec, J. Yu and H. Yersin, *Inorg. Chem.*, 2011, **50**, 8293–8301; (c) Q. Zhang, T. Komino, S. Huang, S. Matsunami, K. Goushi and C. Adachi, *Adv. Funct. Mater.*, 2012, **22**, 2327–2336; (d) X. -L. Chen, R. Yu, Q. -K. Zhang, L. -J. Zhou, X. -Y. Wu, Q. Zhang and C. -Z. Lu, *Chem. Mater.*, 2013, **25**, 3910–3920; (e) M. J. Leitl, F. -R. Kuchle, H. A. Mayer, L. Wesemann and H. Yersin, *J. Phys. Chem. A*, 2013, **117**, 11823–11836; (f) D. M. Zink, M. Bächle, T. Baumann, M. Nieger, M. Kühn, C. Wang, W. Klopfer, U. Monkowius, T. Hofbeck, H. Yersin and S. Bräse, *Inorg. Chem.*, 2013, **52**, 2292–2305; (g) M. J. Leitl, V. A. Krylova, P. I. Djurovich, M. E. Thompson and H. Yersin, *J. Am. Chem. Soc.*, 2014, **136**, 16032–16038; (h) T. Hofbeck, U. Monkowius and H. Yersin, *J. Am. Chem. Soc.*, 2015, **137**, 399–404; (i) M. Osawa, M. Hoshino, M. Hashimoto, I. Kawata, S. Igawa and M. Yashima, *Dalton Trans.*, DOI: 10.1039/c4dt02853h.
- 12 Y. Sakai, Y. Sagara, H. Nomura, N. Nakamura, Y. Suzuki, H. Miyazaki and C. Adachi, *Chem. Comm.*, 2015, **51**, 3181–3184.
- 13 Triazine derivatives as an acceptor, see: (a) A. Endo, K. Sato, K. Yoshimura, T. Kai, A. Kawada, H. Miyazaki and C. Adachi, *Appl. Phys. Lett.*, 2011, **98**, 083302; (b) H. Tanaka, K. Shizu, H. Miyazaki and C. Adachi, *Chem. Commun.*, 2012, **48**, 11392–11394; (c) S. Y. Lee, T. Yasuda, H. Nomura and C. Adachi, *Appl. Phys. Lett.*, 2012, **101**, 093306; (d) H. Tanaka, K. Shizu, H. Nakanotani and C. Adachi, *Chem. Mater.*, 2013, **25**, 3766–3771; (e) H. Tanaka, K. Shizu, H. Nakanotani and C. Adachi, *J. Phys. Chem. C*, 2014, **118**, 15985–15994; (f) S. Hirata, Y. Sakai, K. Masui, H. Tanaka, S. Y. Lee, H. Nomura, N. Nakamura, M. Yasumatsu, H. Nakanotani, Q. Zhang, K. Shizu, H. Miyazaki and C. Adachi, *Nat. Mater.*, 2015, **14**, 330–336; (g) M. Kim, S. K. Jeon, S. -H. Hwang and J. Y. Lee, *Adv. Mater.*, 2015, **27**, 2515–2520.
- 14 Spiro-conjugated systems, see: (a) G. Méhes, H. Nomura, Q. Zhang, T. Nakagawa and C. Adachi, *Angew. Chem. Int. Ed.*, 2012, **51**, 11311–11315; (b) T. Nakagawa, S. -Y. Ku, K. -T. Wong and C. Adachi, *Chem. Commun.*, 2012, **48**, 9580–9582; (c) K. Nasu, T. Nakagawa, H. Nomura, C. -J. Lin, C. -H. Cheng, M. -R. Tseng, T. Yasuda and C. Adachi, *Chem. Commun.*, 2013, **49**, 10385–10387; (d) H. Ohkuma, T. Nakagawa, K. Shizu, T. Yasuda, C. Adachi, *Chem. Lett.*, 2014, **43**, 1017–1019.
- 15 Cyano benzene derivatives as an acceptor, see: (a) H. Uoyama, K. Goushi, K. Shizu, H. Nomura and C. Adachi, *Nature*, 2012, **492**, 234–238; (b) B. Li, H. Nomura, H. Miyazaki, Q. Zhang, K. Yoshida, Y. Suzuma, A. Orita, J. Otera and C. Adachi, *Chem. Lett.*, 2014, **43**, 319–321; (c) M. Taneda, K. Shizu, H. Tanaka and C. Adachi, *Chem. Commun.*, 2015, **51**, 5028–5031; (d) D. R. Lee, S. -H. Hwang, S. K. Jeon, C. W. Lee and J. Y. Lee, *Chem. Commun.*, 2015, **51**, 8105–8107.
- 16 Heptaazaphenylene derivatives as an acceptor, see: (a) J. Li, T. Nakagawa, J. MacDonald, Q. Zhang, H. Nomura, H. Miyazaki and C. Adachi, *Adv. Mater.*, 2013, **25**, 3319–3323; (b) J. Li, Q. Zhang, H. Nomura, H. Miyazaki and C. Adachi, *Appl. Phys. Lett.*, 2014, **105**, 013301.
- 17 Diphenyl sulfone derivatives as an acceptor, see: (a) Q. Zhang, J. Li, K. Shizu, S. Huang, S. Hirata, H. Miyazaki and C. Adachi, *J. Am. Chem. Soc.*, 2012, **134**, 14706–14709; (b) S. Wu, M. Aonuma, Q. Zhang, S. Huang, T. Nakagawa, K. Kuwabara, and C. Adachi, *J. Mater. Chem. C*, 2014, **2**, 421–424; (c) Q. Zhang, B. Li, S. Huang, H. Nomura, H. Tanaka and C. Adachi, *Nat. Photonics*, 2014, **8**, 326–332.
- 18 Diazo derivatives as an acceptor, see: (a) J. Lee, K. Shizu, H. Tanaka, H. Nomura, T. Yasuda and C. Adachi, *J. Mater. Chem. C*, 2013, **1**, 4599–4604; (b) Y. Sagara, K. Shizu, H. Tanaka, H. Miyazaki, K. Goushi, H. Kaji and C. Adachi, *Chem. Lett.*, DOI: 10.1246/cl.141054; (c) H. Tanaka, K. Shizu, J. Lee and C. Adachi, *J. Phys. Chem. C*, 2015, **119**, 2948–2955.
- 19 Benzophenone derivatives as an acceptor, see: (a) S. Y. Lee, T. Yasuda, Y. S. Yang, Q. Zhang and C. Adachi, *Angew. Chem. Int. Ed.*, 2014, **53**, 6402–6406; (b) Q. Zhang, H. Kuwabara, W. J. Potscavage Jr., S. Huang, Y. Hatae, T. Shibata and C. Adachi, *J. Am. Chem. Soc.*, 2014, **136**, 18070–18081; (c) S. Y. Lee, T. Yasuda, I. S. Park and C. Adachi, *Dalton Trans.*, DOI: 10.1039/c4dt03608e.
- 20 J. Lee, K. Shizu, H. Tanaka, H. Nakanotani, T. Yasuda, H. Kaji and C. Adachi, *J. Mater. Chem. C*, 2015, **3**, 2175–2181.
- 21 (a) H. -G. Busmann, H. Staerk and A. Weller, *J. Chem. Phys.*, 1989, **91**, 4098–4105; (b) M. N. Berberan-Santos and J. M. Garcia, *J. Am. Chem. Soc.*, 1996, **118**, 9391–9394; (c) N. J. Turro, V. Ramamurthy and J. C. Scaiano, *Principles of*

- Molecular Photochemistry: An Introduction*, University Science Books, Sausalito, 2008, Chapter 2.
- 22 (a) M. Kinoshita, H. Kita and Y. Shirota, *Adv. Funct. Mater.*, 2012, **12**, 780–786; (b) A. Nagai, S. Kobayashi, Y. Nagata, K. Kokado, H. Taka, H. Kita, Y. Suzuri and Y. Chujo, *J. Mater. Chem.*, 2010, **20**, 5196–5201.
- 23 During the submission of this paper, Adachi et al. also reported luminescent materials bearing 10*H*-phenoxaborin moieties. M. Numata, T. Yasuda and C. Adachi, *Chem. Commun.*, DOI: 10.1039/C5CC00307E.
- 24 Adachi et al. showed how an experimental ΔE_{ST} value was determined from onset of emission, see ref. 18a.
- 25 N. C. Giebink and S. R. Forrest, *Phys. Rev. B: Condens. Matter Mater. Phys.*, 2008, **77**, 235215.
- 26 (a) M. J. Frisch, G. W. Trucks, H. B. Schlegel, G. E. Scuseria, M. A. Robb, J. R. Cheeseman, G. Scalmani, V. Barone, B. Mennucci, G. A. Petersson, H. Nakatsuji, M. Caricato, X. Li, H. P. Hratchian, A. F. Izmaylov, J. Bloino, G. Zheng, J. L. Sonnenberg, M. Hada, M. Ehara, K. Toyota, R. Fukuda, J. Hasegawa, M. Ishida, T. Nakajima, Y. Honda, O. Kitao, H. Nakai, T. Vreven, J. A. Montgomery Jr., J. E. Peralta, F. Ogliaro, M. Bearpark, J. J. Heyd, E. Brothers, K. N. Kudin, V. N. Staroverov, R. Kobayashi, J. Normand, K. Raghavachari, A. Rendell, J. C. Burant, S. S. Iyengar, J. Tomasi, M. Cossi, N. Rega, M. J. Millam, M. Klene, J. E. Knox, J. B. Cross, V. Bakken, C. Adamo, J. Jaramillo, R. Gomperts, R. E. Stratmann, O. Yazyev, A. J. Austin, R. Cammi, C. Pomelli, J. W. Ochterski, R. L. Martin, K. Morokuma, V. G. Zakrzewski, G. A. Voth, P. Salvador, J. J. Dannenberg, S. Dapprich, A. D. Daniels, Ö. Farkas, J. B. Foresman, J. V. Ortiz, J. Cioslowski and D. J. Fox, *Gaussian 09 (Revision D.01)*, Gaussian, Inc., Wallingford CT, 2009. (b) R. Dennington, T. Keith and J. Millam, *GaussView (Version 5)*, Semichem, Inc., Shawnee Mission, KS, 2009.
- 27 (a) R. Bauernschmitt and R. Ahlrichs, *Chem. Phys. Lett.*, 1996, **256**, 454–464; (b) M. E. Casida, C. Jamorski, K. C. Casida and D. R. Salahub, *J. Chem. Phys.*, 1998, **108**, 4439.
- 28 (a) S. Huang, Q. Zhang, Y. Shiota, T. Nakagawa, K. Kuwabara, K. Yoshizawa and C. Adachi, *J. Chem. Theory Comput.*, 2013, **9**, 3872–3877; (b) T. Chen, L. Zheng, J. Yuan, Z. An, R. Chen, Y. Tao, H. Li, X. Xie, W. Huang, *Sci. Rep.*, 2015, **5**, 10923.
- 29 C. Ganzoring and M. Fujihira, *Appl. Phys. Lett.*, 2002, **81**, 3137–3139.
- 30 (a) E. Dimitrijević and M. S. Taylor, *Chem. Sci.*, 2013, **4**, 3298–3303; (b) L. Niu, H. Yang, Y. Jiang and H. Fu, *Adv. Synth. Catal.*, 2013, **355**, 3625–3632.
- 31 J. H. Cho, Y. -S. Ryu, S. H. Oh, J. K. Kwon and E. K. Yum, *Bull. Korean Chem. Soc.*, 2011, **32**, 2461–2464.
- 32 S. N. Bagriantsev, K. -H. Ang, A. Gallardo-Godoy, K. A. Clark, M. R. Arkin, A. R. Renslo and D. L. Minor Jr., *ACS Chem. Biol.*, 2013, **8**, 1841–1851.